A Summary of the Hanford Single-Shell Tank Structural Analysis of Record [a] - 15526

Ken I. Johnson*, John E. Deibler*, Naveen K. Karri*, Scott E. Sanborn*,
F. George Abatt**, Ken L. Stoops**, Larry J. Julyk**, Brian M. Larsen**,
*Pacific Northwest National Laboratory, Richland, Washington 99352
** Becht Engineering Co., Inc., Richland, Washington 99352

ABSTRACT

Washington River Protection Solutions, LLC (WRPS), the USDOE Hanford Site tank contractor, developed an enhanced Single-Shell Tank Integrity Project (SSTIP) in 2009 to better understand the integrity of the single-shell tanks (SSTs). A panel of experts from industry and academia was created to recommend project activities in four main areas: structural integrity, liner degradation, leak integrity and prevention, and contamination migration. One of the panel's primary recommendations was to perform a detailed structural integrity analysis of the SSTs. WRPS and the U.S. Department of Energy, Office of River Protection commissioned the Pacific Northwest National Laboratory (PNNL) to perform this structural integrity analysis of record for the Hanford single shell tanks. This is one of seventeen panel recommendations that form the M-45-10-1 Change Package for the Hanford Federal Agreement and Compliance Order; also known as the Tri-Party Agreement.

Finite element analysis was used to predict the structural response of the SSTs to the historical thermal and operating loads, plus design basis seismic loads. Bounding thermal histories were established from waste temperature records and applied to the model to include the thermal degradation of concrete modulus and strength, plus cracking due to differential thermal expansion while under in situ static loading conditions. PNNL contracted with Becht Engineering to evaluate the dynamic response of the tanks to a design basis earthquake. The degraded stiffness of the reinforced concrete was also incorporated in the seismic analysis. The combined response to static and seismic loads was then evaluated against the design requirements of the American Concrete Institute standard, ACI-349-06, for nuclear safety-related concrete structures. Specific analyses were performed for the four major tank designs. This paper presents an overview of the analysis methods used and it summarizes the major analytical findings that are common to the tanks and others that are specific to the individual tank designs. The analyses of record determined that including the bounding effects of their operating histories, each tank design currently satisfies the ACI-349-06 structural integrity design requirements. Although leak tightness is not directly addressed in the structural integrity analysis, this analysis will be a key input in the formal tank integrity assessment due in 2018.

INTRODUCTION

The 149 Hanford underground single shell tanks (SSTs) were constructed between the 1940's and the 1960's for temporary storage of radioactive waste material. The four tank types described in Table I range in capacity from 208 m^3 (55,000 gal) to 3,785 m^3 (1,000,000 gal). The smallest Type I tanks are 6

---

[a] This manuscript has been authored by Battelle Memorial Institute, Pacific Northwest Division, under Contract No. DE-AC06-76RL0 1830 with the U.S. Department of Energy. The publisher, by accepting the article for publication, acknowledges that the United States Government retains a non-exclusive, paid-up, irrevocable, world-wide license to publish or reproduce the published form of this manuscript, or allow others to do so, for United States Government purposes.

m (20 ft) in diameter while the Type II, III, and IV tanks are 23 m (75 ft) in diameter (Figure 1). The SST analysis of record (AOR) project began by reviewing the historical operating data to define the maximum temperature and waste load histories for each tank type. Bounding structural analyses were conducted for each tank type, beginning with the largest number of tanks (Type II) and proceeding to the smallest number (Type I) to evaluate the largest number of tanks with each subsequent analysis [1, 2, 3, 4]. The Type IVB design was chosen to represent the Type IV tanks based on a comparative analysis of the Type IVA, IVB, and IVC designs. The Type IVC (AX-Farm) design was also analyzed in detail to evaluate the structural interaction of tanks that are closely spaced.

TABLE I. Classification of single-shell tanks.

| Type	Farms	Tank Size	Years of Construction	Total
I	B, C, T, and U	200-series, 6-m Φ, 208 m^3 (20-ft Φ, 55,000 gal)	1943-1944	16
II	B, C, T, and U BX	100-series, 23-m Φ, 1893 m^3 (75 ft Φ, 500,000 gal)	1943-1944 1947-1948	60
III	S, BY, TX, and TY	100-series, 23-m Φ, 2840 m^3 (75 ft Φ, 750,000 gal)	1947-1952	48
IVA	SX	100-series, 23-m Φ, 3785 m^3 (75 ft Φ, 1,000,000 gal)	1953-1955	15
IVB	A	100-series, 23-m Φ, 3785 m^3 (75 ft Φ, 1,000,000 gal)	1953-1956	6
IVC	AX	100-series, 23-m Φ, 3785 m^3 (75 ft Φ, 1,000,000 gal)	1963-1965	4
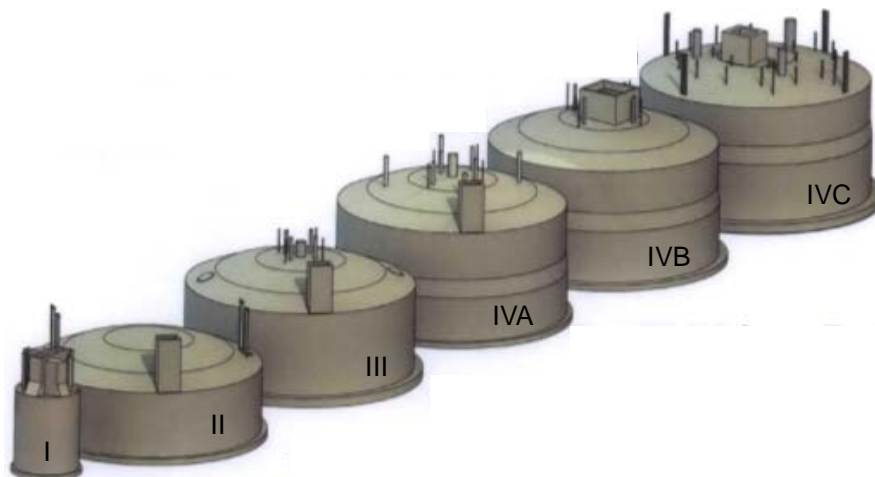
Figure 1. Single-Shell Tank Configurations

The SST analysis of record was performed to ASME-NQA-1 quality standards [5]. The engineering analysis methods used in the tank structural integrity evaluations are described in the Evaluation Criteria report [6]. The American Concrete Institute (ACI) code ACI-349-06, *Code Requirements for Nuclear Safety Related Concrete Structures* [7] provides the tank acceptance criteria for the AOR. The primary focus of the ACI code is to evaluate the reinforced concrete tank structure under combined flexure and

axial loads. Dead loads, live loads, fluid, thermal, and seismic loads are all considered. Material degradation due to temperature and aging was also included.

The ACI evaluation demonstrates tank structural integrity based on the design code limits. However, determining the load-capacity margin to collapse requires a more detailed analysis, because the loads can redistribute under progressive failure such that the maximum load capacity exceeds the code limit. The dome limit load analyses therefore used nonlinear analysis with concrete crushing and cracking plus rebar yielding to estimate the margin between the ACI design code capacity and the higher dome collapse load. Buckling analyses were also performed to address the ACI code requirement to evaluate the stability of thin shell concrete structures. This paper summarizes the engineering methods used in the SST analysis of record and the major conclusions from that analysis.

ANALYSIS OF THERMAL AND OPERATING LOADS

Detailed thermal and structural models were developed from the construction drawings of each tank design using the ANSYS® finite element code [8]. The ANSYS® SOLID65 (3-D Reinforced Concrete Solid) elements were used to represent concrete regions with and without reinforcement bars (rebars). SOLID65 elements include features to simulate concrete cracking in tension, crushing in compression, and creep. The reinforced concrete is divided into regions that have different steel reinforcement ratios. The 25 mm (1 in.) thick reinforcement layers ("rebar elements" in Figure 2) were located in the cross-section thickness to accurately model the bending resistance of the reinforcing bars. The reinforcement model in the SOLID65 elements is a smeared model where the amount of steel in each element is specified as a volume fraction of the total element volume. The volume fraction of reinforcing steel is modeled as an elastic-plastic material. The soil surrounding the tank is modeled with SOLID185 elements, with the Extended Drucker-Prager material model used to simulate the pressure dependent yield behavior of the Hanford soils. The nonlinear contacts at the concrete to soil interface use TARGE170 and CONTA173 elements. The thermal model uses the same finite element mesh with ANSYS® SOLID70 heat transfer elements.
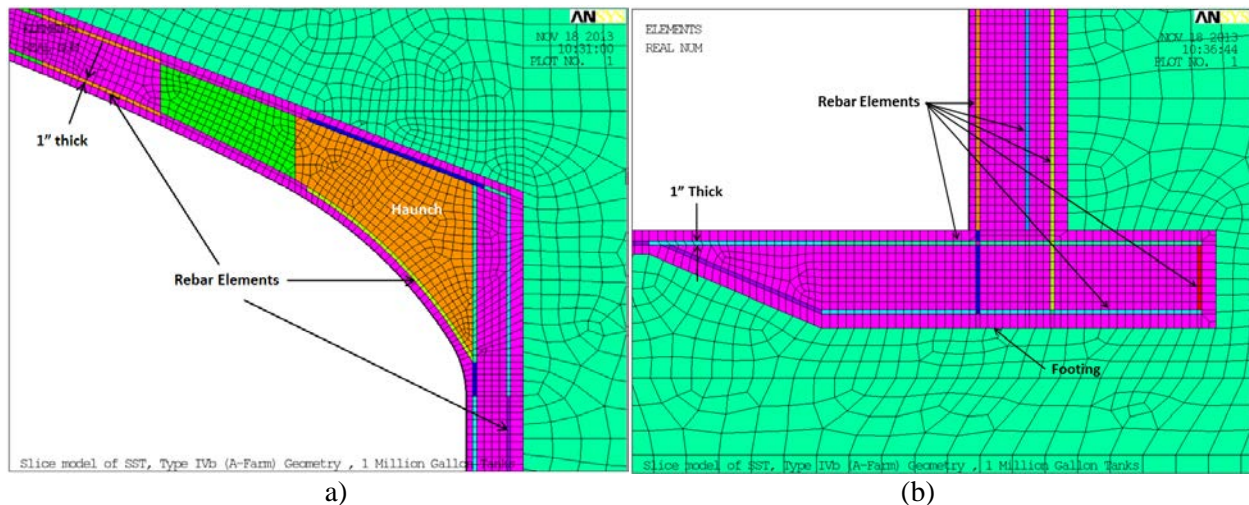

Figure 2. (a) Close-Up of Haunch (a) and Footing (b) Showing the Soil and Reinforced Concrete Elements of the Type IVB Thermal and Operating Loads Tank Model.

The thermal and operating loads analysis (TOLA) considers the following mechanical live and dead loads: a) The maximum soil overburden depth for each tank type with a soil density of 2,000 kg/m^3 (specific weight of 125 lbf/ft^3), b) hydrostatic loads due to waste (variable depth at specific gravity of 1.7) applied as pressure loads on the inner surface of the tank, c) a 1,915 Pa (40 lbf/ft^2) uniform surface live load to account for snow and ash fall, and d) the maximum concentrated live load allowed by the current dome load control program applied uniformly over a 6 m (20 ft) diameter circular area centered over the tank dome or roof at the soil surface for the 100-series and the 200-series tanks, respectively. The mechanical loads were applied progressively (gravity loads, the initial waste load, and the surface live loads) followed by the transient thermal loads from the heat transfer analysis.

The historical tank farm operating records provided valuable information on the temperature distributions during high temperature events such as the self-boiling of high heat wastes. The temperature data from the AX tank farm were particularly valuable because these tanks include thermocouple tubes cast into the inner and outer walls of the tank. The inside and outside wall temperatures taken at three heights in the AX tank walls consistently showed that the maximum wall temperatures remained in the 99°C (210°F) to 121°C (250°F) range at the same time when the maximum waste temperature reached 282°C (540°F) near the center of the tank floor region. Hanford historical documents also report that the boiling point of the SST liquid wastes was in the range of 104°C (220°F) to 121°C (250°F). These temperatures are consistent with a concentration of high-heat solids near the floor center with boiling and convective flow bringing the hot liquid to the surface and the cooler liquid flowing down the walls transferring heat outward to the soil (Figure 3). Evidence that the maximum wall and footing temperatures did not exceed 121°C (250°F) is significant to tank structural integrity, because it suggests that thermal degradation of the concrete strength and stiffness is also limited in the footing and wall by the moderate temperatures that were reached there. This is also consistent with the recent sidewall coring of tank A-106 (the highest temperature tank), which produced cores with compressive strengths well above the 20 MPa (3 ksi) design strength throughout the height of the wall core [9].
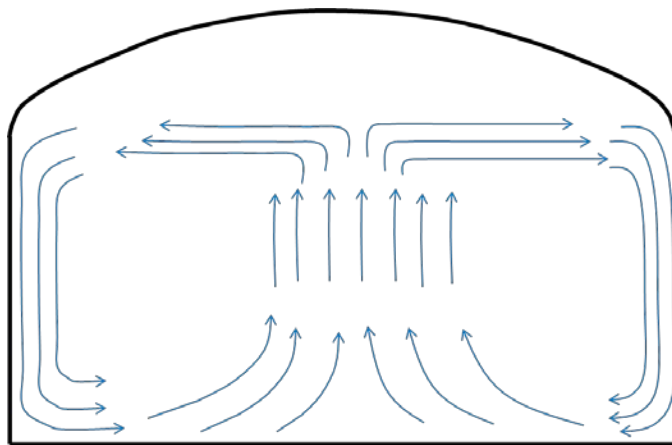

Figure 3. The Estimated Convective Flow Pattern of Self-Boiling Liquid Waste

The TOLA run matrix included seven different combinations of soil modulus, concrete modulus/strength and creep to bound the uncertainties in material properties. Several additional studies, e.g. shear friction at construction joints, alternate ACI load factors, and waste height sensitivity, were also conducted.

ANALYSIS OF SEISMIC LOADS

The soil-structure interaction (seismic) models were created and analyzed in the time domain using version 13.0 of the general-purpose finite element program ANSYS® [8]. The Evaluation Criteria [6] defined the maximum considered earthquake (MCE) ground motions as the ground motions with a mean annual exceedance frequency of 1 in 2500 years (2% probability of exceedance in 50 years). In this analysis, the site-specific design response spectra (DRS) for the SST facilities site uses the Hanford Waste Treatment Plant (WTP, located in the 200 East area) design spectra as a reasonable assessment of the current state of knowledge of the hazard levels at the Hanford 200 East and 200 West areas where the SSTs are located. Because the SSTs are designated as Performance Category 2 (PC-2) structures, the SST ground motions are developed as 2/3 of the Hanford Site MCE ground motion.

The seismic run matrix included nine different combinations of three soil profiles, two waste levels, and two waste moduli to encompass the variety of configurations and bound uncertainties in material properties. Additional analysis studies were conducted to validate modeling techniques and investigate sources of sensitivity. These studies were performed using selected subsets of the model configurations.

A half-symmetry (180°) model of the SST, including the concrete tank and surrounding soil, was developed to evaluate the soil-structure interaction response of the tank (see Figure 4). The tank concrete was modeled with ANSYS® SHELL181 (4-node finite strain shell) elements at the mid-line profile of the tank cross-section. The soil and tank contents are modeled with ANSYS® SOLID45 linear elastic volumetric elements.
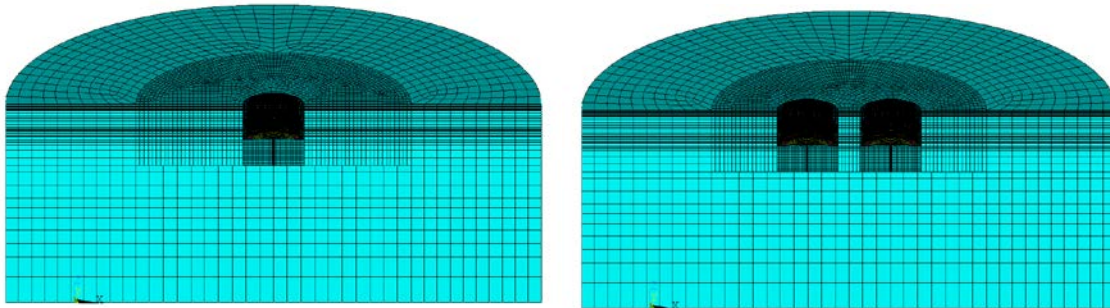

Figure 4. Single- and Two-Tank (Tank-to-Tank Interaction) ANSYS Models

The seismic model includes both backfill soil properties and far-field soil properties. As required by ASCE [10], the seismic analysis includes lower bound, best estimate, and upper bound soil properties to account for uncertainties in the soil properties. Each set of soil properties has its own material properties, soil layering and depth, and seismic input motion.

The concrete properties assigned to the models are degraded properties developed from the TOLA analysis. The tanks were evaluated in either an empty or nearly full tank configuration so that worst case loadings would be captured. Because the current SST waste consists of saltcake and sludge-like material, the waste was modeled using low stiffness elastic volumetric elements.

The seismic model includes ANSYS® CONTA173 and TARGE170 contact interfaces between the tank and the surrounding soil, between the tank waste and the inner surface of the tank wall, and within the soil above the tank dome. The contacts are allowed to slide and separate at the interface between the tank and

the soil, and are allowed to slide but not separate between the tank wall and the tank contents or within the soil. The contact interfaces constitute the only nonlinearities in the seismic model.

Contacts are used in the soil above the tank dome to prevent or minimize soil arching. In the seismic models, vertical contact surfaces are inserted into the overburden to create annular rings of soil that are free to displace vertically with the tank roof, but allow the load to transfer laterally during horizontal motion. This effectively creates a nonlinear yield mechanism that acts in the vertical direction only. The effectiveness of this technique was demonstrated by matching the theoretical at-rest soil pressure on the dome.

Additional mass is added to the soil surface above the dome to simulate concentrated loads such as tank pits and permanent or temporary equipment. The magnitude of the mass is applied in accordance with the Hanford tank dome load controls.

A lateral boundary distance of at least 97.5 m (320 ft) was chosen based on spectral matching of the model boundary spectra with the free-field spectra at the corresponding elevation. All nodes on the periphery of the model have been "slaved" to a single node at each layer to force the soil to behave essentially as a shear beam. The soil depth is selected in accordance with ASCE [10] such that the shear wave velocity at the base is greater than or equal to 1,067 m/s (3,500 ft/s), or else the base is at least three times the maximum foundation dimension below the foundation.

The free-field seismic model input motion developed for the AOR of each tank type using SHAKE [11] was calibrated for use in ANSYS® through spectral matching to ensure that the ANSYS® soil-structure-interaction (SSI) model reproduced or bounded the corresponding free-field response at the tank foundation elevation and at the soil surface. Calibration was necessary because SHAKE operates in the frequency domain and ANSYS® operates in the time domain. Thus, factors such as damping and boundary conditions operate differently between the two programs. Spectral matching criteria were used to ensure that the spectra corresponding to the ANSYS® input seismic acceleration time series appropriately matched the SHAKE target spectra. This resulted in a conservative margin between the ANSYS® seismic response spectra and the corresponding SHAKE target spectra. The margin is particularly significant for frequencies above 2.5 Hz for the horizontal ground motion and above 8 Hz for the vertical ground motion. Therefore, the reported seismic demands are likely to be conservative by 20-40% as shown in Figure 5.
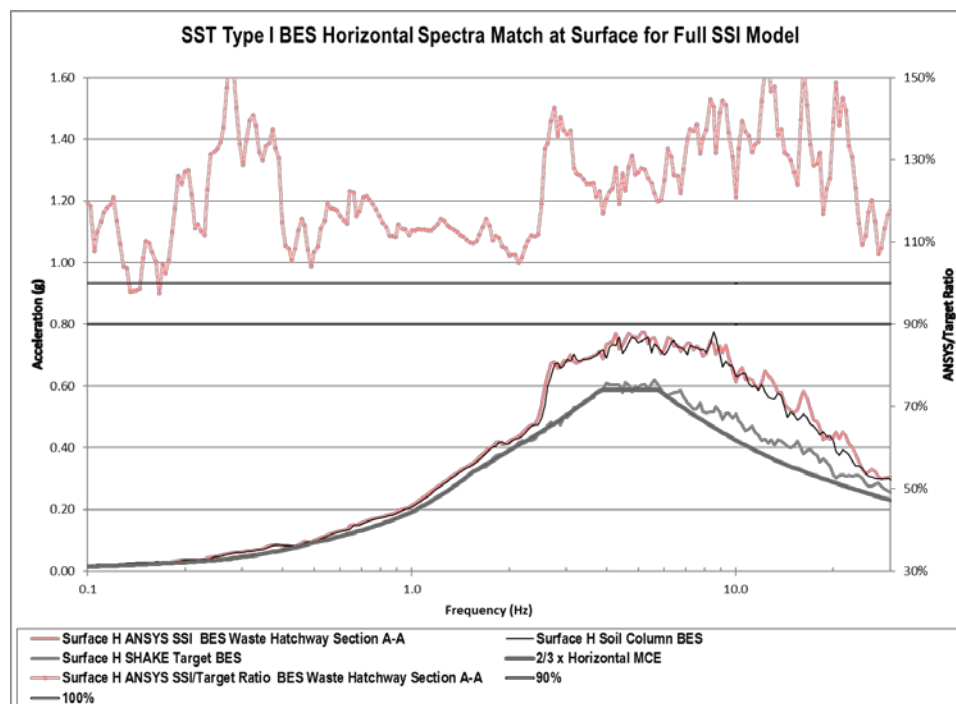
Figure 5. Comparison of Best Estimate Horizontal Surface Spectra from the ANSYS® SSI Model
(Typical for all SST types)

A large point mass element (more than 100 times the mass of the full model) is located at the base of the model and the seismic excitation is applied at that node as a transient force corresponding to the known acceleration at the base of the model. All nodes at the base elevation of the model are coupled to the point mass to create a rigid region. Because the ANSYS SSI model has a rigid base that will reflect downward propagating waves, the prescribed input motions are the in-column motions generated by the program SHAKE. The in-column motions are appropriate because they represent the superposition of both the upward and downward propagating waves at the location of the rigid boundary.

Two-directional seismic excitation is applied as horizontal excitation parallel to the symmetry plane and vertical excitation. The horizontal excitation consists of vertically propagating (horizontal) shear waves and the vertical excitation consists of vertically propagating compression waves. Both directions of input are applied simultaneously. Loading is applied to the model in two steps; initial gravity, and seismic excitation. The initial gravity step establishes the proper geostatic conditions for the subsequent nonlinear seismic evaluation. The deadweight plus seismic forces and moments obtained from the SSI analysis are extracted from the tank concrete elements and post-processed to produce seismic-only resultant tank section loads throughout the tank structure. The post-processing uses an enveloping process to produce bounding seismic loads that are conservative in space (circumferentially) and time.

EVALUATION OF ACI-349-06 LOAD COMBINATIONS

Section 9.2 of the ACI-349-06 code [7] defines an extensive list of load combinations that must be considered in evaluating reinforced concrete structures. Of these combinations, ACI-349-06 load combinations 1, 4, and 9 are appropriate for the SST structural integrity evaluations. These factored load combinations are defined as follows:

Load Combination 1 (LC1).	$U = 1.4D + 1.4F + 1.7L + 1.7H$	(1)
Load Combination 4 (LC4).	$U = D + F + L + H + T_o + E_{ss}$	(2)
Load Combination 9 (LC9).	$U = 1.05D + 1.05F + 1.3L + 1.3H + 1.05T_o$	(3)

These equations define the section demands (U) as factored combinations of dead loads (D), live loads (L), fluid pressure loads (F), loads due to adjacent soil pressure (H), thermal loads (T_o), and seismic loads (E_{ss}). The scale factors were applied to the loads (rather than to the model results) so that nonlinear concrete cracking is correctly included for increased loads. The ACI evaluation was also performed with unfactored loads at the time of maximum temperature to ensure that the concrete section capacities were not exceeded such as to invalidate the continuum assumption of the finite element model. If section capacities were exceeded, then shear failure planes or locally degraded stiffnesses would have to be included at those locations.

Figure 6 shows the tank sections where the ACI demand vs. capacity evaluations were performed for the Type IV tanks. The ACI sections begin at the center of the dome and traverse through the haunch, down the wall, and back across the bottom slab. The sections were defined similarly for the other tank analyses. Force-moment interaction diagrams (also shown in Figure 6) of all sections were developed to define the ACI section capacities. The demand/capacity ratio (D/C) is defined as the ratio of the vector length from the origin to the force-moment demand coordinate to the vector length from the origin to the capacity curve assuming that the same ratio of force to moment would be maintained. D/C ratios less than or equal to 1.0 indicate that the ACI design basis requirements are met. The actual margin is more difficult to assess if the same ratio of force to moment is not maintained.
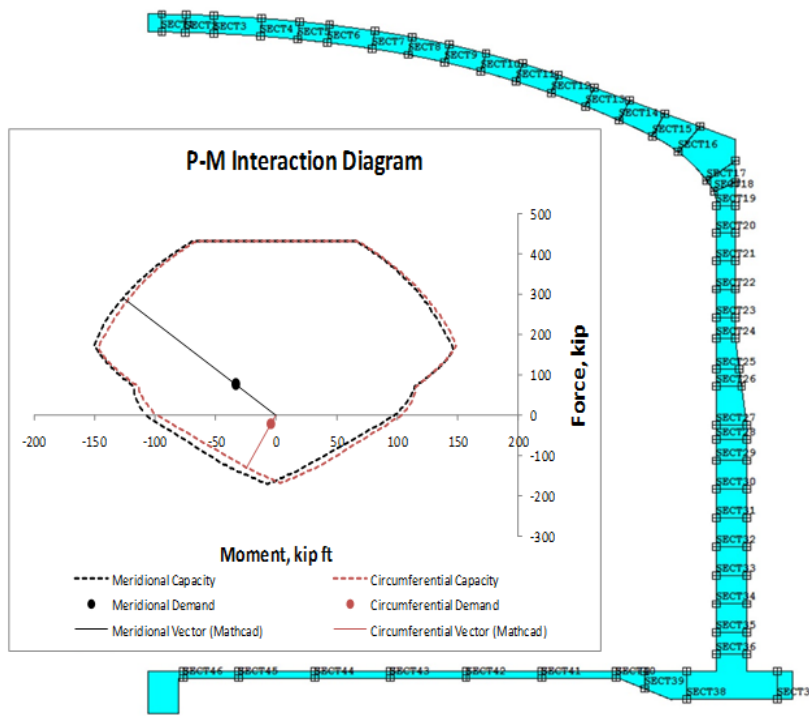

Figure 6. Type IV SST ACI Evaluated Section Locations and an Example P-M Interaction Diagram for Evaluating Combined Axial (P) and Moment (M) Section Loads

The LC1, LC4, and LC9 load combinations were evaluated for a matrix of best estimate, lower-bound and upper-bound material property combinations. The combinations were also evaluated for meridional loads, circumferential loads, through-thickness shear, and in-plane shear loads. Figure 7 shows an example of the D/C ratios for the Type IV, LC1 through-section shear evaluation. This plot shows that the D/C ratios are less than 1.0 for all sections and material property combinations in the tank. An important finding of the SST AOR was that the D/C ratios for the LC1, LC4, and LC9 evaluations are all less than 1.0 in the roof, haunch, and wall for all of the material and load combinations evaluated for each of the four tank types.
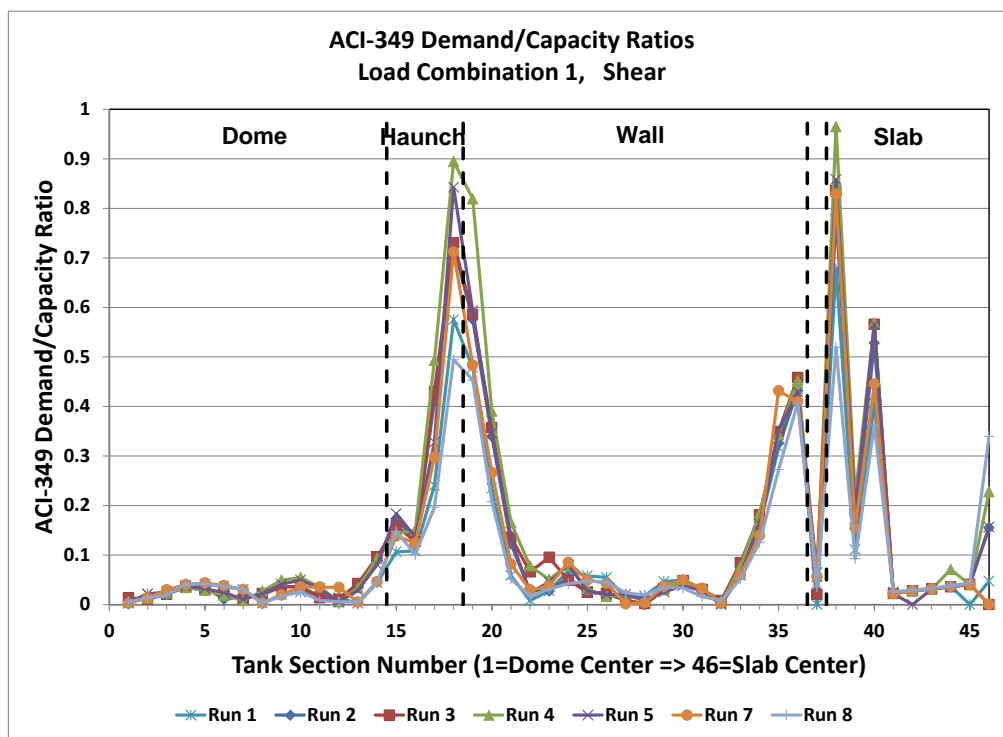

Figure 7. Type IV SST Through-Wall Shear ACI D/C Ratios for Load Combination 1

Figure 8 shows another example of the Type IV meridional loads evaluation at the peak temperature condition. In this case, some locations in the bottom slab inboard of the footing do have D/C ratios greater than 1.0. This finding was also noted for the other tank types under peak temperatures. This indicates that crushing and cracking of the slab may have occurred from radial thermal expansion followed by contraction under the bounding thermal histories. However, the bottom slab is supported on soil, and the cracking and displacements are displacement-controlled. Cracks in the bottom slab do not affect the structural stability of the tank dome, walls, and footing.
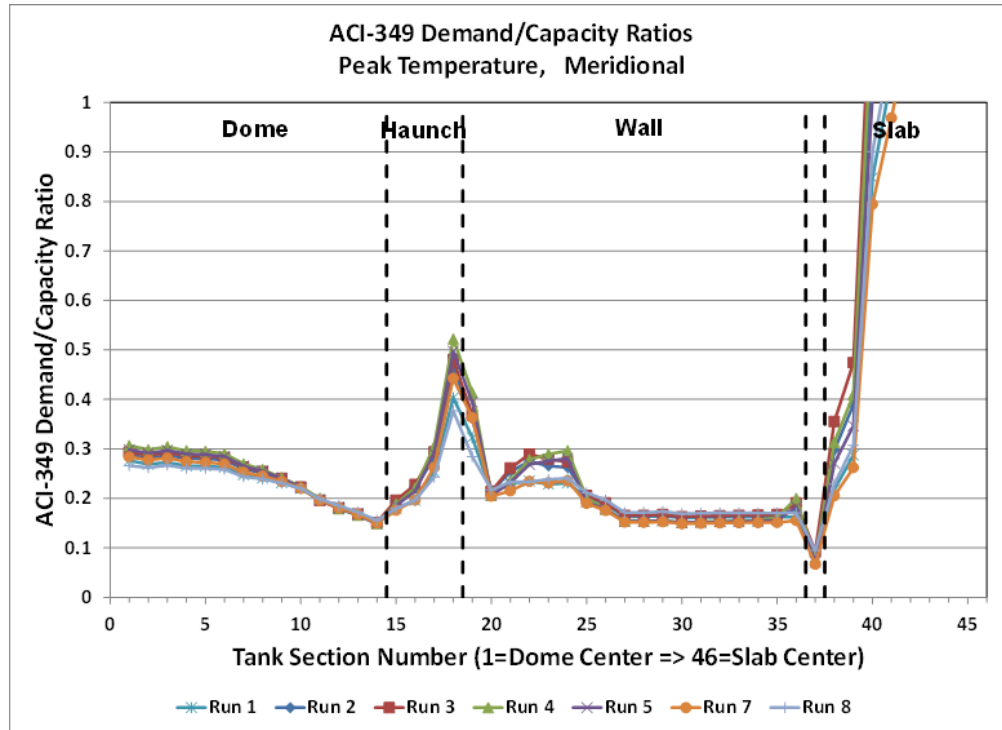
Figure 8. Type IV Tank, Meridional ACI D/C Ratios at Peak Temperature

Additional finite element analyses were performed with the bottom slab separated from the tank footing to further evaluate the effect of possible cracking and shear offset of the concrete at this location (Figure 9). Note also that Figure 7 shows an example where the maximum LC1 shear D/C ratio (0.96) is close to the ACI-349-06 capacity in the bottom slab just inboard of the footing (section 38). The slab separation studies demonstrated that even in the event of local slab shear failure, the slab-to-footing offset deformation was predicted to be less than one-half of the nominal thickness of the steel tank bottom. Therefore, it is expected that the steel liner would bridge the small displacement offset without being damaged. The conclusion from the slab separation analysis is that exceeding the ACI design load capacity in the bottom slab does not affect the structural stability of the tanks.
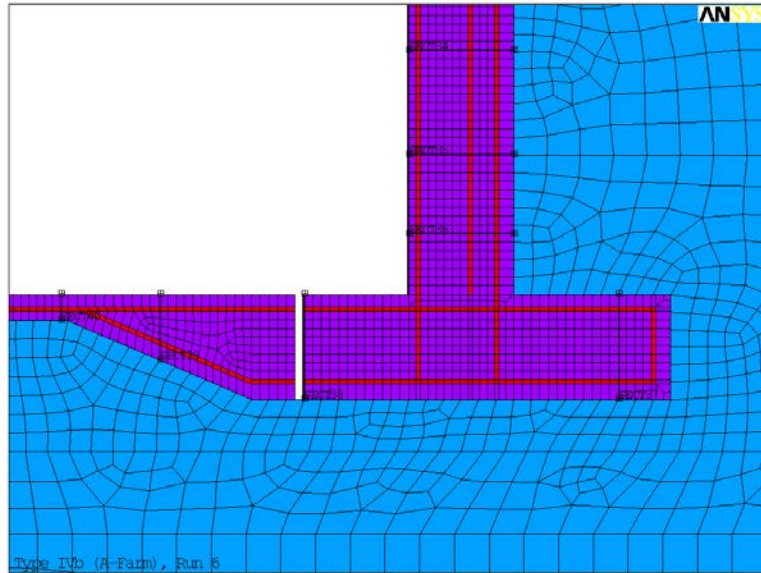
Figure 9. The Slab Detached from the Footing to Assess Differential Settlement

LIMIT LOAD AND BUCKLING ANALYSES

Tank dome limit load analyses was conducted to estimate the margin between the current maximum dome load limits and the collapse load limits. The thermal and operating load histories were applied to the static finite element models to establish the present day conditions of the tanks; including the effects of concrete thermal degradation, cracking, and creep. Additional surface loads were then applied until the tank structures offered little or no resistance to further load. The tank dome limit loads were evaluated for both the in situ uniform soil-load condition and for operating loads concentrated over the center of the tank domes. The effect of additional soil or surface barrier material was determined by applying a uniform pressure over the entire soil surface. The limit loads for local concentrated operating loads were approximated by applying a local pressure on the soil surface over a 6 m (20 ft) diameter circular area above the tank center. These loads were individually increased until concrete crushing or rebar yielding finally occurred. The corresponding calculated dome collapse limit loads were more than three times the current dome load limits, demonstrating that adequate margin exists between the current dome load limits and the maximum dome load capacities.

The SST evaluation also considered buckling of both the dome and walls of the four tank types. Tank dome buckling was approximated from solutions for a spherical cap under both uniform and locally applied pressure loads. Buckling of the tank wall was assessed for axial loads and external pressure loads. The effects of construction tolerances, inelastic behavior, creep, reinforcement, and cracking were considered when estimating buckling load reduction factors for application to the theoretical buckling loads. The analysis methods were based on procedures recommended by the ACI for concrete shell structures [12]. The buckling analyses consistently demonstrated safety factors greater than specified in the Evaluation Criteria report [6]. Therefore, tank buckling is not predicted to occur.

STRUCTURAL INTERACTION OF CLOSELY SPACED TANKS

The AOR models used for the tank evaluations consist of single-tank models. Most of the 23 m (75 ft) diameter SSTs are positioned in arrays with a center-to-center spacing of 31 m (102 ft), so that adjacent tanks are separated by soil that extends more than 50% of the tank radius. However, the four AX farm

tanks have an East-West spacing of only 27 m (90 ft), which gives a tank-to-tank separation of only 28% of the tank radius. Therefore, a tank-to-tank interaction (TTI) study was conducted to evaluate the structural interaction of these closely spaced tanks and to determine if any adjustments are required to the single-tank models to account for TTI effects [13]. Detailed finite element models with two adjacent tanks were developed to evaluate the variation of thermal, operating, and seismic loads around the perimeter of the tanks (Figure 10). The results from single-tank and two-tank models (with 27m (90 ft) and 31m (102 ft) center-to-center spacings) were compared to develop guidelines for adjusting single-tank model results to account for the close proximity of adjacent tanks. Structural sensitivity studies were also performed for variations in waste depth, soil coefficient of thermal expansion, and temperature histories. The D/C ratios of the two-tank and single-tank models were compared for ACI-349-06 load combinations 1 and 4.
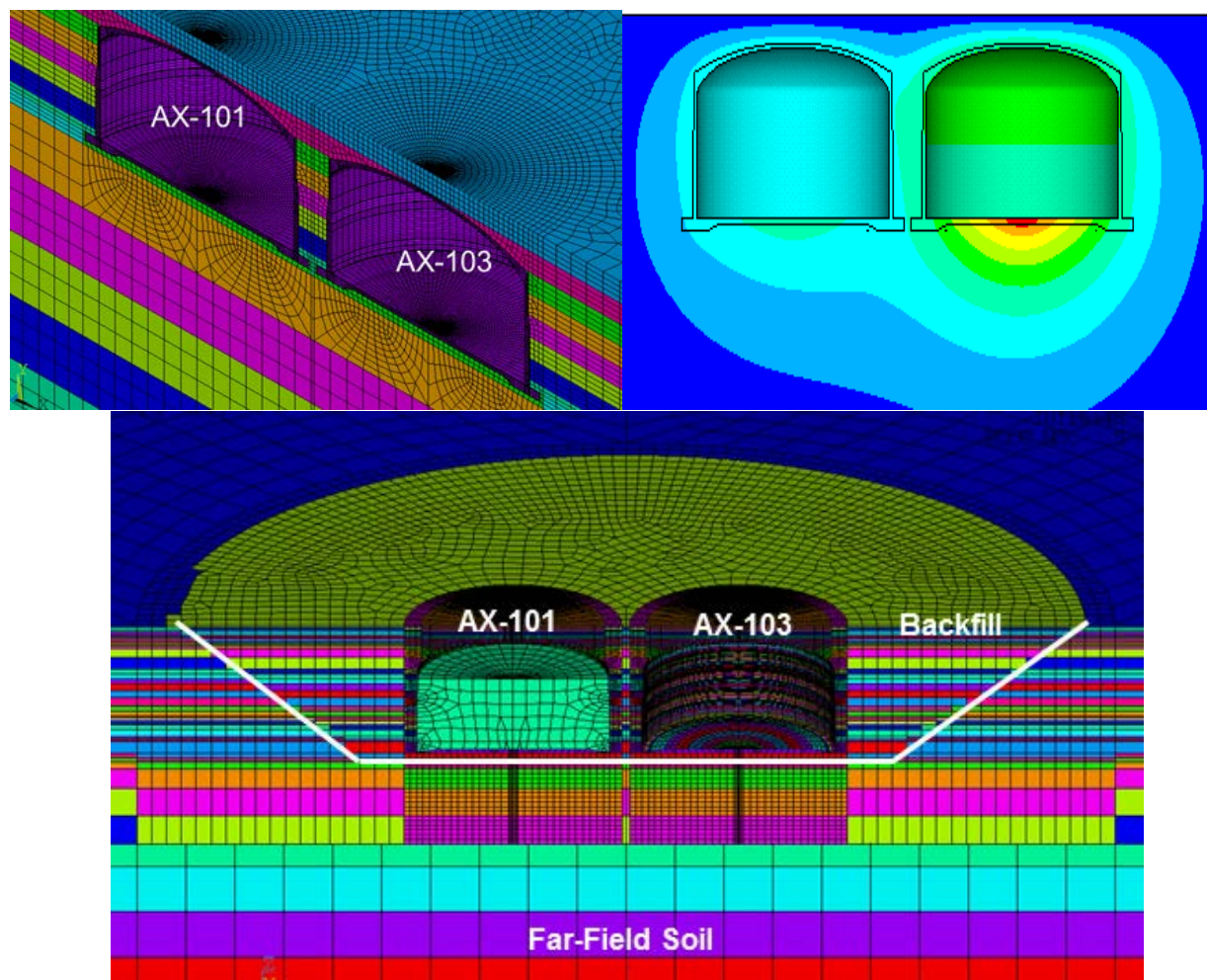

Figure 10. The Structural, Thermal, and Seismic Models Used in the Tank-to-Tank Interaction Study

The thermal and operating loads analyses show that loads in certain areas of the tank are increased as the tanks are positioned closer and closer together. The maximum D/C ratios around the circumference of the tank were almost always higher for the 27m (90 ft) tank spacing than for the 31 m (102 ft) spacing, and both were generally higher than the single-tank results. However, the differences between the 27 m (90 ft) and 31 m (102 ft) spacings are small.

In general, higher concrete seismic demands occur when the tanks are closer together and when the difference in waste depth (mass) is greater. Thus, the greatest concrete seismic demands occur when one empty and one full tank are most closely spaced. When the waste depths (masses) are more closely matched in adjacent tanks (which is the typical case in the Hanford SST farms), the effects of TTI are less. The seismic demands were combined with the thermal and operating loads to evaluate the LC4 load combination D/C ratios.

The two-tank results are not significantly different from the single-tank results at most section locations around the tank cross-section. Three dimensional plots of the TTI D/C ratios over the 180^0 tank models indicate that the ratios are typically greater than the single tank ratios within the 30° arc where the neighboring tanks are the closest (a 60° total arc centered about the closest point between tanks). Enveloping the TTI results over all azimuthal locations showed that the single-tank D/C ratios generally fall between the maximum and minimum TTI D/C ratios at peak temperature and LC1 conditions. It is also important to note that the maximum D/C ratios for the dome, haunch, walls, and outer footing were less than 0.85 for all of the analysis cases run in the TTI study of the Type IVC tanks. The TTI effects increase the D/C ratios by ≤0.1 for most conditions, with a few specific conditions where the maximum TTI effect increases the single-tank D/C ratios by up to 0.2. Therefore, single tank D/C ratios less than 0.8 satisfy the ACI evaluation criteria without a detailed TTI evaluation. Tank sections with single tank D/C ratios greater than 0.8 can be evaluated by applying the TTI factors summarized in [13] for specific locations and loads.

CONCLUSIONS

This paper describes the engineering methods and results of the Hanford SST updated analyses of record. Detailed structural analyses were performed to ASME-NQA-1 quality standards for each of the four major SST design types. The bounding thermal, operating, and seismic loads analyses for each tank type do not reveal any deficiencies with the Hanford SSTs that jeopardize their structural integrity. While the analyses do indicate that the SST concrete bottom slabs are likely damaged from high temperature exposure, they also demonstrate that this damage will not affect the overall stability or structural integrity of the tanks.

Evidence that the maximum wall and footing temperatures did not exceed 121°C (250°F) is significant to tank structural integrity, because it suggests that thermal degradation of the concrete strength and stiffness is also limited in the footing and wall by the moderate temperatures that were reached there. This is also consistent with the recent sidewall coring of tank A-106 (the highest temperature tank), which produced cores with compressive strengths well above the 20 MPa (3 ksi) design strength throughout the height of the wall core [9].

The soil overburden is the largest load on the tank and the largest contributor to the static tank demands. The waste and loads on the soil surface produced only secondary effects. Thermal loads were significant in the bottom slab and lower wall where the temperatures were highest. The material combination of upper bound concrete modulus and lower bound soil modulus increased both the TOLA and seismic concrete section demands.

Softer soil tends to create the greatest seismic demands overall, and stiffer soil tends to create the least seismic demands overall. The seismic demands are all small compared to the TOLA demands even including the estimated 20-40% conservatism in the seismic input accelerations. The greatest seismic

loads typically occur in the haunch, and seismic demands in the floor are small relative to other locations. The dome is sensitive primarily to the soil configuration and insensitive to the waste configuration. The wall demands are most sensitive to waste configuration and soil stiffness. The highest seismic demands in the wall occur for a nearly full tank with the higher modulus (stiff) waste. The lowest seismic demands in the wall occur for an empty tank. The in-plane shear forces in the wall show more sensitivity to the soil stiffness than other seismic demands. Through-wall shear forces typically peak near the haunch and the footing. The hoop forces in the wall show more sensitivity to the waste height and stiffness than other seismic demands.

The influence of TTI on seismic demands is complex. The tank spacing, the waste height differences, and the differences in concrete properties between two interacting tanks all have an observable effect on concrete seismic demands. In some cases the difference in demands between a full and empty tank is as important a variable as tank spacing. Although the differences in TTI seismic demands are large on a percentage basis, the seismic demands are small compared to the thermal and operating loads (which also include TTI effects). When the D/C ratios are calculated the effect of the TTI seismic differences is minimized by the higher TOLA loads.

The TTI study showed that the two-tank D/C ratios are similar to the single-tank ratios, with the largest differences occurring near the bottom of the walls between neighboring tanks. The maximum TTI effects add ≤ 0.2 to the D/C ratios from the analogous single tank model, and the difference between 27 m (90 ft) and 31m (102 ft) TTI effects is small. Therefore, single tank D/C < 0.8 will satisfy the ACI-349-06 criteria without detailed TTI evaluation. It was also noted that the largest TTI differences do not occur where the maximum D/C ratios occur in the single tank model analyses. So, while TTI effects are evident in the tank analyses, they are not the dominant contributor to the highest D/C ratios of the Type IVC (AX) analysis. This conclusion supports the use of single-tank models in performing the SST analyses of record.

ACKNOWLEDGEMENT

REFERENCES

1. Rinker MW, KI Johnson, SK Bapanapalli, NK Karri, JE Deibler, SP Pilli, CE Guzman-Leong, SE Sanborn, FG Abatt, JA Dewberry, BM Larsen, KL Stoops, and LJ Julyk. 2011. *Single-Shell Tank Integrity Project Analysis of Record: Hanford Type II Single-Shell Tank Thermal and Operating Loads and Seismic Analysis*. RPP-RPT-49989, Rev. 0, Pacific Northwest National Laboratory, Richland, Washington.

2. Rinker MW, KI Johnson, SK Bapanapalli, NK Karri, JE Deibler, SP Pilli, CE Guzman-Leong, SE Sanborn, FG Abatt, JA Dewberry, BM Larsen, KL Stoops, and LJ Julyk. 2011. *Single-Shell Tank Integrity Project Analysis of Record: Hanford Type III Single-Shell Tank Thermal and Operating Loads and Seismic Analysis*. RPP-RPT-49990, Rev. 0, Pacific Northwest National Laboratory, Richland, Washington.

3. Johnson KI, SP Bapanapalli, JE Deibler, FG Abatt, KL Stoops, NK Karri, SE Sanborn, SP Pilli, BM Larsen and LJ Julyk. 2014. *Single-Shell Tank Integrity Project Analysis of Record: Hanford Type IV Single-Shell Tank Thermal and Operating Loads and Seismic Analysis*. RPP-RPT-49992, Rev. 0; PNNL-23341, Rev. 0, Pacific Northwest National Laboratory, Richland, Washington.

4. Johnson KI, SP Bapanapalli, JE Deibler, FG Abatt, KL Stoops, NK Karri, SE Sanborn, SP Pilli, BM Larsen and LJ Julyk. 2014. *Single-Shell Tank Integrity Project Analysis of Record: Hanford Type I Single-Shell Tank Thermal and Operating Loads and Seismic Analysis*. RPP-RPT-49993, Rev. 0; PNNL-23745, Rev. 0, Pacific Northwest National Laboratory, Richland, Washington.

5. ASME 2000, *Quality Assurance Requirements for Nuclear Facility Applications*, ASME NQA-1 2000, American Society of Mechanical Engineers, New York, NY.

6. Johnson KI, JE Deibler, FG Abatt, and MW Rinker. 2010. *Single-Shell Tank Structural Evaluation Criteria.* RPP-46442, Rev. 0, Pacific Northwest National Laboratory, Richland, Washington.

7. ACI. 2007. *American Concrete Institute Code Requirements for Nuclear Safety Related Concrete Structures*. ACI 349-06, American Concrete Institute, Farmington Hills, Michigan.

8. ANSYS 2010, *User's Manual Version 13.0*, ANSYS, Inc., Canonsburg, PA.

9. Misiak TA. 2014. *Concrete Core Testing Report for the Single-Shell Tank 241-A-106 Sidewall Coring Project.* RPP-RPT-58254, Rev. 0. U.S. Department of Energy, Richland, Washington.

10. ASCE 2000. *Seismic Analysis of Safety-Related Nuclear Structures and Commentary*, ASCE 4-98. American Society of Civil Engineers, Reston, Virginia.

11. Schnabel, PB, Lysmer, J, and Seed, HB. 1972. *SHAKE – A Computer Program for Earthquake Response Analysis of Horizontally Layered Sites*. Earthquake Research Center, University of California, Berkeley, CA, EERC 72-12.

12. ACI. 1981. *Concrete Shell Buckling*. ACI SP-67, EP Popov and SI Medwadowski (eds). American Concrete Institute (ACI), Detroit, Michigan.

13. Johnson KI, SP Bapanapalli, JE Deibler, FG Abatt, KL Stoops, NK Karri, SE Sanborn, SP Pilli, BM Larsen and LJ Julyk. 2014. *Single-Shell Tank Integrity Project Analysis of Record: Tank to Tank Interaction Study of the Hanford Single-Shell Tanks*. RPP-RPT-49991, Rev. 0; PNNL-23328, Rev. 0, Pacific Northwest National Laboratory, Richland, Washington.